International Journal of Scientific Research and Engineering Development-– Volume 9 Issue 2, Mar-Apr 2026
Available at www.ijsred.com

RESEARCH ARTICLE OPEN ACCESS

Enhancing Solar Power Generation Through Real-Time IoT-Based Single-Axis Tracking

Muhammed Rufai [1], Abdulmumin Umar Saidu [2] and Bilyamin Muhammad[2,3]
[1](Department of Electrical and Electronics Engineering, Kaduna Polytechnic)
[2](Department of Computer Engineering, Kaduna Polytechnic)
3(Department of Computer Engineering, Ahmadu Bello University, Zaria)

----------**********----------

Abstract:

This study presents the design, implementation, and evaluation of a low-cost IoT-enabled single-axis solar tracking system using a 20W photovoltaic panel. The system employs Light Dependent Resistors (LDRs) for sunlight detection, an ESP8266 NodeMCU microcontroller for control, and an L298N motor driver to adjust panel orientation along the east–west axis, with the Blynk IoT platform providing real-time monitoring and remote manual control. Experimental measurements were conducted under natural sunlight at Kaduna Polytechnic, Kaduna State, Nigeria, comparing the tracking system with a fixed panel under identical environmental conditions. Results indicate that the tracking panel consistently outperformed the fixed configuration, achieving a mean power output of 15.92W versus 12.36W and a total daily energy harvest of 101Wh compared to 78Wh, representing approximately a 30% improvement. Graphical analysis showed a broader high-performance window, while statistical validation demonstrated a higher performance ratio (84% versus 65%) and lower standard deviation, reflecting more consistent energy capture. The findings confirm that IoT-enabled solar tracking enhances photovoltaic efficiency and provides a scalable, reliable, and economically viable solution for small- and medium-scale renewable energy applications.

Keywords — Blynk IoT platform; energy efficiency; LDR sensors; photovoltaic energy; single-axis solar tracker

----------**********----------

1. INTRODUCTION

The growing global demand for reliable and sustainable energy has intensified the search for alternative energy sources capable of reducing dependence on fossil fuels [1]. Rapid population growth, industrialization, and technological advancement have significantly increased energy consumption worldwide, leading to environmental challenges such as greenhouse gas emissions and climate change [2]. In response, renewable energy technologies have gained widespread attention, with solar energy emerging as one of the most promising and accessible solutions. According to the International Energy Agency, global solar photovoltaic (PV) capacity surpassed 1,291 gigawatts in 2023, reflecting the rapid adoption of solar technologies across residential, commercial, and industrial sectors [3].

Solar photovoltaic systems convert sunlight directly into electrical energy through the photovoltaic effect. Their performance, however, is highly dependent on the intensity of solar irradiance and the angle at which sunlight strikes the panel surface. Maximum power generation occurs when solar rays are perpendicular to the panel [1]. Conventional fixed solar panels are typically installed at predetermined tilt angles and remain stationary throughout the day [4]. While this design is simple and cost-effective, it does not account for the continuous movement of the sun across the sky. As a result, fixed panels experience

significant energy losses during early morning and late afternoon periods when the angle of incidence deviates from the optimal position [5].

Solar tracking systems have been developed to address this limitation by dynamically adjusting the orientation of solar panels to follow the sun's trajectory. Studies have shown that single-axis tracking systems can improve energy output by approximately 20–30%, while dual-axis systems may achieve even higher gains [6]. Despite these advantages, many commercially available tracking systems are expensive and mechanically complex, limiting their adoption in small-scale or resource-constrained environments [7]. Furthermore, several traditional tracking systems lack remote monitoring and control capabilities, making maintenance and performance evaluation more difficult [8].

Recent advancements in microcontroller technology and the Internet of Things (IoT) have opened new opportunities for developing cost-effective and intelligent solar tracking solutions [9]. IoT integration enables real-time data monitoring, remote control, performance analytics, and improved system management [10]. Low-cost Wi-Fi-enabled microcontrollers such as the ESP8266 allow solar tracking systems to communicate with cloud platforms, providing users with live operational data through smartphones or web applications [11].

This study focuses on the design and implementation of an IoT-enabled solar tracking system aimed at optimizing solar energy harvesting efficiency. The system utilizes Light Dependent Resistor (LDR) sensors to detect sunlight direction, an ESP8266 NodeMCU microcontroller for data processing and decision-making, and a DC motor controlled through an L298N driver to adjust panel orientation. Additionally, the Blynk IoT platform is integrated to enable real-time remote monitoring and manual control of the solar panel system.

2. RELATED STUDIES

Recent advances in photovoltaic (PV) systems emphasize integrated solutions combining mechanical tracking, sensor-based detection, and IoT-enabled monitoring. Mousazadeh et al. [12] reviewed sun-tracking methods, showing significant energy gains over fixed panels, while Duffie and Beckman [13] reported 20–30% improvement for single-axis and up to 40% for dual-axis trackers, highlighting cost and maintenance concerns [14].

Embedded microcontrollers have enabled smart tracking. Kumar and Singh [15] developed a low-cost Arduino-based tracker with improved energy output, but without IoT integration, whereas Gupta et al. [16] used ESP8266 for remote energy monitoring, focusing on visualization rather than active tracking. Al-Ali et al. [17] proposed IoT-based energy management frameworks, though not specific to solar trackers.

Wu et al. [18] implemented a dual-axis tracker using dual GPS receivers, an inclinometer, and the Solar Position Algorithm, achieving energy gains up to 113.7% in mobile scenarios. While highly accurate, the system is complex and costly. Baouche et al. [19] validated a single-axis tracker through simulation and field tests at 36.261° latitude, demonstrating improved efficiency and reduced cost, but with limited real-time control and location generality. Shang and Shen [6] designed a dual-axis photoelectric tracker, achieving 24.6% more energy than a fixed panel, though mechanical complexity remained high.

However, the proposed study adopts a simpler single-axis, LDR-based IoT tracking system using an ESP8266 microcontroller, emphasizing low cost, reduced complexity, real-time adaptive tracking, and remote monitoring while still achieving significant energy improvement over fixed systems.

3. SYSTEM DESIGN

The proposed system is designed as a single-axis solar tracking mechanism integrated with IoT monitoring capability. The system architecture consists of three major subsystems:

i. Sensing Subsystem – Responsible for detecting sunlight intensity using Light Dependent Resistors (LDRs).
ii. Control Subsystem – Built around the ESP8266 microcontroller, which processes sensor data and determines motor movement.

iii. Actuation Subsystem – Comprising the L298N motor driver and DC motor that physically rotate the solar panel.

Additionally, an IoT communication layer enables remote monitoring and manual control through the Blynk

3.1 Sensing Subsystem

The sensing subsystem constitutes the primary input stage of the proposed IoT-enabled solar tracking system. Its main function is to detect variations in solar irradiance and determine the direction of maximum sunlight intensity. The subsystem provides real-time feedback to the control unit, thereby enabling continuous adjustment of the solar panel orientation.

The subsystem is implemented using four Light Dependent Resistors (LDRs) arranged in differential pairs. The sensors are positioned on the solar panel structure and separated by small vertical barriers to ensure directional sensitivity. When the panel is not aligned with the sun, one LDR in a pair receives higher illumination than the other, resulting in a measurable electrical difference. This differential arrangement enhances tracking accuracy and directional discrimination.

3.1.1 Electrical Modeling of the LDR

The LDR operates based on the principle of photoconductivity, where its resistance decreases as incident light intensity increases. The relationship between light intensity E and LDR resistance R_{LDR} can be approximated using Equation (1).

$$R_{LDR} = kE^{-\alpha} \tag{1}$$

Where:
k is a proportionality constant
α is a material constant (typically between 0.7 and 0.9)
E is the incident light intensity

Under high illumination, R_{LDR} decreases significantly, while under low illumination it increases.

3.1.2 Voltage Divider Configuration

Each LDR is connected in series with a fixed resistor R_f to form a voltage divider circuit. The output voltage supplied to the microcontroller's analog input is expressed Equation (2).

$$V_{out} = V_{in} \times \frac{R_{LDR}}{R_f + R_{LDR}} \tag{2}$$

Where:
V_{in} is the supply voltage
R_f is the fixed resistor
R_{LDR} is the light-dependent resistance

As light intensity varies, the change in R_{LDR} produces a corresponding change in output voltage, which is converted into digital form through the Analog-to-Digital Converter (ADC) of the microcontroller.

3.1.3 Differential Light Intensity Measurement

The directional tracking decision is based on the voltage difference between opposing LDR pairs. The voltage difference is calculated using Equation (3).

$$\Delta V = V_1 - V_2 \tag{3}$$

The system initiates corrective movement when:

$$|\Delta V| > V_{th}$$

Where:
V_{th} is a predefined threshold voltage to prevent unnecessary oscillation due to minor fluctuations.

If:

$$|\Delta V| \leq V_{th}$$

the panel is considered optimally aligned and no motor action is taken.

3.1.4 Solar Incidence Consideration

The effectiveness of solar energy harvesting depends on minimizing the angle of incidence θ between incoming sunlight and the panel surface. The effective irradiance I_{eff} is governed by the cosine law presented Equation (4).

$$I_{effective} = I\cos(\theta) \tag{4}$$

The sensing subsystem indirectly minimizes θ by continuously adjusting the panel orientation toward the direction of maximum detected illumination.

3.1.5 Signal Stabilization

To improve measurement stability and reduce mechanical wear caused by rapid motor switching, signal conditioning techniques are incorporated. The system may employ sample averaging presented in Equation (5).

$$V_{avg} = \frac{1}{n}\sum_{i=1}^{n} V_i \tag{5}$$

Where:
n is the number of ADC samples.

Additionally, a short delay interval is introduced between successive readings to ensure stable decision-making.

3.2 Control Subsystem

The control subsystem serves as the central processing and decision-making unit of the proposed IoT-enabled solar tracking system. It receives input signals from the sensing subsystem, processes the data using a predefined control algorithm, and generates appropriate output signals to the actuation subsystem. In addition, it manages wireless communication for real-time monitoring and remote interaction.

The control unit is built around the ESP8266 NodeMCU microcontroller. This microcontroller integrates processing capability, memory resources, input/output interfaces, and built-in Wi-Fi connectivity within a single compact module. Its architecture allows simultaneous handling of sensing, control, and communication tasks, thereby simplifying system design and reducing hardware complexity.

3.2.1 Signal Processing and ADC Conversion

The analog voltage signals obtained from the voltage divider circuits are converted into digital form using the built-in Analog-to-Digital Converter (ADC). The digital output value D corresponding to an input voltage V_{in} is given by Equation (6).

$$D = \frac{V_{in}}{V_{ref}} \times (2^n - 1) \tag{6}$$

Where:
V_{ref} = reference voltage of the ADC
n = ADC resolution in bits
D = digital output value

The digitized sensor readings are then used in the tracking algorithm for directional comparison.

3.2.2 Control Algorithm

The decision-making logic is based on differential comparison of sensor readings. The control conditions are defined as:

- If $\Delta V > V_{th}$, rotate motor in one direction.
- If $\Delta V <- V_{th}$, rotate motor in the opposite direction.
- If $|\Delta V| \leq V_{th}$, stop motor.

This threshold-based approach prevents unnecessary oscillations caused by minor fluctuations in light intensity.

The algorithm operates in a continuous loop with a small delay interval t_d to stabilize system response.

3.2.3 PWM-Based Motor Speed Control

To ensure smooth mechanical movement, the control subsystem can implement Pulse Width Modulation (PWM) for motor speed regulation. The effective motor voltage V_{eff} under PWM control is expressed using Equation (7).

$$V_{eff} = D_c \times V_s \quad (7)$$

Where:
D_c = duty cycle (0–1)
V_s = supply voltage

By adjusting the duty cycle, the controller regulates motor speed, thereby reducing mechanical stress and improving positioning accuracy.

3.3 Actuation Subsystem

The actuation subsystem is responsible for converting electrical control signals into mechanical motion to adjust the orientation of the solar panel. It forms the output stage of the closed-loop solar tracking system and ensures that the panel is physically aligned toward the direction of maximum solar irradiance as determined by the control subsystem.

The subsystem consists of a 12V DC motor mechanically coupled to the solar panel mounting structure and interfaced through an L298N dual H-bridge motor driver module. The integration of the motor and driver enables controlled bidirectional rotation of the panel along a single axis (east-west direction).

3.3.1 DC Motor Modeling

A DC motor operates based on electromagnetic principles, converting electrical energy into mechanical rotational motion. The fundamental voltage equation of a DC motor is given by Equation (8).

$$V = E_b + I_a R_a \quad (8)$$

Where:
V = applied voltage
E_b = back electromotive force (EMF)
I_a = armature current
R_a = armature resistance

The back EMF is proportional to angular velocity as presented in Equation (9).

$$T = k_t I_a \quad (9)$$

Where:
k_t = torque constant
I_a = armature current

These equations indicate that motor speed and torque can be controlled by adjusting the applied voltage and current.

3.3.2 Motor Driver Operation (L298N)

The L298N motor driver module serves as an interface between the low-power microcontroller and the higher-power DC motor. It operates using an H-bridge configuration that allows bidirectional current flow through the motor.

Motor direction control is achieved as follows:

- Input 1 = HIGH, Input 2 = LOW → Clockwise rotation
- Input 1 = LOW, Input 2 = HIGH → Counterclockwise rotation
- Both LOW or both HIGH → Motor stop

The driver also supports Pulse Width Modulation (PWM) for speed control through its enable pin.

3.3.3 Mechanical Coupling and Torque Requirement

The motor is mechanically connected to the solar panel mounting frame using a gear mechanism. The gearbox reduces rotational speed while increasing torque, ensuring sufficient force to rotate the panel structure under load conditions.

The required torque T_{req} to rotate the panel is determined by Equation (10).

$$T_{req} = F \times r \quad (10)$$

Where:
F = force due to panel weight and friction
r = radius of rotation

The selected motor and gearbox combination ensures that the developed torque exceeds T_{req} for reliable operation.

3.4 Performance Metrics

To evaluate the effectiveness of the solar tracking system, several performance metrics were employed. These metrics quantify energy output, efficiency, consistency, and deviation from ideal performance. Each metric is defined below along with its calculation method.

Mean Power Output: The mean power output represents the average power generated by a system over the observation period. It provides a simple measure of overall performance, and it is computed using Equation (11).

$$\bar{P} = \frac{\sum_{i=1}^{n} P_i}{n} \tag{11}$$

Where P_i is instantaneous power at time *I,* and *n* is the total number of measurements.

Standard Deviation (σ): Standard deviation measures the variability of the power output around the mean value. It indicates the consistency and stability of energy generation. it computed using Equation (12).

$$\sigma = \sqrt{\frac{\sum_{i=1}^{n}(P_i - \bar{P})^2}{n}} \tag{12}$$

Where $\bar{P}$ is the mean power.

Performance Ratio (PR): The performance ratio quantifies the efficiency of a solar panel system relative to its rated (maximum theoretical) energy output, computed using Equation (13).

$$PR(\%) = \frac{\text{Actual Energy Output}}{\text{Rated Energy Output}} \times 100 \tag{13}$$

Where the Actual Energy Output is the measured daily energy generation, and the Rated Energy Output is the theoretical maximum energy the panel could generate under ideal conditions.

Energy Yield (E_{total}): Energy yield represents the total electrical energy produced by a panel over the measured period. It is computed using Equation (14).

$$E_{\text{total}} = \sum_{i=1}^{n} P_i \cdot \Delta t \tag{14}$$

Where Δt is the sampling interval (h).

4. RESULTS AND DISCUSSION

This section presents and analyzes the performance of the developed IoT-enabled single-axis solar tracking system using a 20 W photovoltaic (PV) panel. All measurements were conducted under natural sunlight conditions at Kaduna Polytechnic, Kaduna, Nigeria. The analysis compares the developed solar tracking system with a fixed solar panel under identical environmental conditions, focusing on voltage, current, instantaneous power, daily energy yield, and statistical performance metrics.

4.1 Experimental Conditions

The system was tested over five consecutive days under predominantly clear skies between 8:00 AM and 5:00 PM, with measurements taken at one-hour intervals. The fixed panel was mounted at an optimized tilt angle suitable for the location, while the tracking panel rotated along the east–west axis in response to light intensity detected by LDR sensors. Both systems experienced identical environmental conditions to ensure fair comparison.

4.2 Performance of the Fixed Solar Panel

The fixed 20 W panel exhibited maximum power of 19.00 W at 12:00 PM, with a gradual decline in the morning and late afternoon (Table 1). The average power output was 12.36 W, corresponding to a daily energy yield of 78 Wh. The narrow peak around midday highlights the limitation of fixed panels under varying solar angles.

Table -1: Fixed Solar Panel Output

Time	Voltage (V)	Current (A)	Power (W)
8:00 AM	14.2	0.58	8.24
10:00 AM	17.5	0.85	14.88
12:00 PM	18.1	1.05	19.00
2:00 PM	17.8	0.98	17.44
4:00 PM	15.3	0.60	9.18
5:00 PM	13.6	0.40	5.44

4.3 Performance of the Solar Tracking Panel

The single-axis tracking panel continuously aligned with the sun along the east–west axis, achieving higher output throughout the day (Table 2). The peak power of 22.30 W at 12:00 PM exceeded the panel's nominal rating under optimal alignment. Average power across the day was 15.92 W, resulting in an estimated daily energy yield of 101 Wh. The broader power profile demonstrates the tracking system's ability to extend productive energy generation into morning and late afternoon hours.

Table -2: Solar Tracking Panel Output

Time	Voltage (V)	Current (A)	Power (W)
8:00 AM	16.0	0.75	12.00
10:00 AM	18.2	1.02	18.56
12:00 PM	18.9	1.18	22.30
2:00 PM	18.5	1.12	20.72
4:00 PM	16.8	0.82	13.78
5:00 PM	14.8	0.55	8.14

4.4 Comparative Analysis

Table 3 presents the power output of both panels, highlighting improvements achieved by the tracking system.

Table -3: Comparative Power Output

Time	Fixed Panel (W)	Tracking Panel (W)	Improvement (W)	Improvement (%)
8:00 AM	8.24	12.00	3.76	45.6
10:00 AM	14.88	18.56	3.68	24.7
12:00 PM	19.00	22.30	3.30	17.4
2:00 PM	17.44	20.72	3.28	18.8
4:00 PM	9.18	13.78	4.60	50.1
5:00 PM	5.44	8.14	2.70	49.6

4.4.1 Evaluation Using Mean Power Output

The mean power output was 12.36 W for the fixed panel and 15.92 W for the tracking panel, representing a 29–30% improvement. Fig. 1 illustrates the instantaneous power versus time, showing that the fixed panel peaks sharply around midday, while the tracking panel exhibits a broader, elevated curve throughout the day, confirming extended high-performance hours.

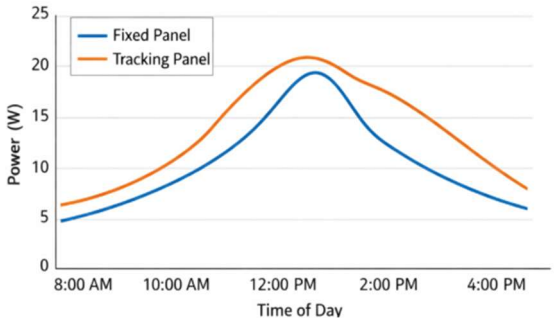

Fig. -1: Power vs Time for Fixed and Tracking Panels

Fig. 2 compares total daily energy harvested, with the tracking panel achieving 101Wh versus 78Wh for the fixed panel, visually confirming the ~30 % increase in daily energy yield.

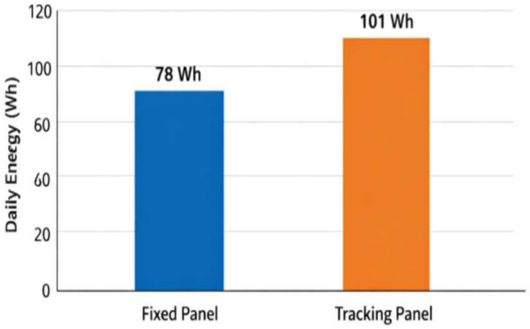

Fig. -2: Daily Energy Comparison between Fixed and Tracking Panels

4.4.2 Evaluation Using Standard Deviation (σ)

The tracking system demonstrated a slightly lower standard deviation (5.08 W) compared to the fixed panel (5.31 W), indicating more consistent energy output throughout the day, particularly during early morning and late afternoon periods.

Table -4: Mean Power and Standard Deviation

Panel Type	Mean Power (W)	Standard Deviation (W)
Fixed	12.36	5.31
Tracking	15.92	5.08

4.4.3 Evaluation Using Performance Ratio (PR)

The tracking panel achieved a higher performance ratio of 84 %, compared to 65 % for the fixed panel, reflecting improved energy utilization and reduced losses due to suboptimal alignment.

Table -5: Performance Ratio

Panel Type	Actual Energy (Wh)	Rated Energy (Wh)	PR (%)
Fixed	78	120	65
Tracking	101	120	84

The comparative analysis confirms that the IoT-enabled single-axis tracking system improves mean power, daily energy yield, and output consistency over a fixed panel, particularly in early morning and late afternoon hours, without introducing operational instability.

5. CONCLUSIONS

The IoT-enabled single-axis solar tracking system effectively maximized energy capture through continuous panel alignment with sunlight. Experimental results showed extended power generation beyond midday, with notable improvements in early morning and late afternoon performance. The tracking mechanism operated reliably under natural sunlight, responding accurately to irradiance changes without electrical instability or mechanical oscillations. Compared to a fixed panel, the system achieved higher mean power, greater daily energy yield, and improved efficiency, with a lower standard deviation and higher performance ratio, indicating consistent operation. These findings demonstrate that low-cost, IoT-integrated tracking systems offer a practical and scalable solution for enhancing photovoltaic energy utilization in small- and medium-scale applications.

ACKNOWLEDGEMENT

The authors wish to express their sincere gratitude to the Directorate of Research and Development, Kaduna Polytechnic, for their support and guidance throughout this project; appreciation is also extended to TETFund for sponsoring the research, enabling the successful implementation and evaluation of the IoT-enabled solar tracking system

REFERENCES

[1] M. Suleiman, D. K. Joshi, B. Muhammad, and I. Bello, "Performance improvement of PV modules under the effect of partial shading using bil-bot wiping mechanism," *Int. J. Recent Eng. Res. Dev.*, vol. 9, no. 04, pp. 108–116, 2024.

[2] A. Rehman, M. M. Alam, I. Ozturk, R. Alvarado, M. Murshed, Ç. Işık, and H. Ma, "Globalization and renewable energy use: how are they contributing to upsurge the CO2 emissions? A global perspective," *Environ. Sci. Pollut. Res.*, vol. 30, no. 4, pp. 9699–9712, 2023.

[3] M. O. Levin, "Conserving power considering animal movement around large-scale, ground-mounted photovoltaic solar energy facilities in the United States," Columbia Univ., 2025.

[4] S. Alam, A. Qadeer, and M. Afazal, "Determination of the optimum tilt-angles for solar panels in Indian climates: A new approach," *Comput. Electr. Eng.*, vol. 119, p. 109638, 2024.

[5] S. Satheesh, S. Venkat, and R. B. Mulford, "Optimization of panel spacing, tilt angle and azimuth angle for bifacial panels with fixed land acreage and orientation for several United States locations," in *Proc. ASME Int. Mech. Eng. Congr. Expo.*, vol. 87899, p. V001T09A003, 2024.

[6] H. Shang and W. Shen, "Design and implementation of a dual-axis solar tracking system," *Energies*, vol. 16, no. 17, p. 6330, 2023.

[7] A. Badawi, I. M. Elzein, W. Alqaisi, C. El-Bayeh, M. Al-Kuwari, A. Al-Marri, … and W. Ghanem, "Design and experimental evaluation of an affordable dual-axis solar tracker for off-grid applications," *Int. J. Robot. Control Syst.*, vol. 5, no. 6, pp. 3147–3167, 2025.

[8] R. Sadeghi, M. Parenti, S. Memme, M. Fossa, and S. Morchio, "A review and comparative analysis of solar tracking systems," *Energies*, vol. 18, no. 10, p. 2553, 2025.

[9] D. C. Nath, I. Kundu, A. Sharma, P. Shivhare, A. Afzal, M. E. M. Soudagar, and S. G. Park, "Internet of things integrated with solar energy applications: a state-of-the-art review," *Environ., Dev. Sustain.*, vol. 26, no. 10, pp. 24597–24652, 2024.

[10] M. S. Yahya, B. Muhammad, M. A. Abubakar, U. I. Abdullahi, and Z. I. Musa, "Implementation of a real-time IoT based energy management system," *J. Eng. Res. Rep.*, vol. 25, no. 10, pp. 19–29, 2023.

[11] N. S. Mitu, V. Vassilev, and M. R. Tabany, "Low cost, easy-to-use, IoT and cloud-based real-time environment monitoring system using ESP8266 microcontroller," *Int. J. Internet Things Web Serv.*, vol. 6, pp. 30–44, 2021.

[12] H. Mousazadeh, A. Keyhani, A. Javadi, H. Mobli, K. Abrinia, and A. Sharifi, "A review of principle and sun-tracking methods for maximizing solar systems output," *Renew. Sustain. Energy Rev.*, vol. 13, no. 8, pp. 1800–1818, 2009.

[13] J. A. Duffie and W. A. Beckman, *Solar Engineering of Thermal Processes*, 4th ed. Hoboken, NJ, USA: Wiley, 2013.

[14] S. A. Kalogirou, *Solar Energy Engineering: Processes and Systems*, 2nd ed. London, UK: Academic Press, 2014.

[15] P. Kumar and R. Singh, "Design and implementation of Arduino-based solar tracking system," *Mater. Today: Proc.*, vol. 45, pp. 3205–3211, 2021.

[16] S. Gupta, R. Sharma, and A. Kumar, "IoT-based energy monitoring system using ESP8266," *Int. J. Energy Res.*, vol. 43, no. 7, pp. 3176–3185, 2019.

[17] A. R. Al-Ali, I. Zualkernan, and F. Aloul, "A smart home energy management system using IoT and big data analytics approach," *IEEE Trans. Consum. Electron.*, vol. 65, no. 4, pp. 371–379, 2019.

[18] C. H. Wu, H. C. Wang, and H. Y. Chang, "Dual-axis solar tracker with satellite compass and inclinometer for automatic positioning and tracking," *Energy Sustain. Dev.*, vol. 66, pp. 308–318, 2022.

[19] F. Z. Baouche, B. Abderezzak, A. Ladmi, K. Arbaoui, G. Suciu, T. C. Mihaltan, … and F. E. Țurcanu, "Design and simulation of a solar tracking system for PV," *Appl. Sci.*, vol. 12, no. 19, p. 9682, 2022.

